

# Design and realization of a portable Edge Illumination X-ray Phase Contrast imaging system

D. Basta,<sup>1, a)</sup> M. Endrizzi,<sup>1</sup> F. A. Vittoria,<sup>1,2</sup> G. K. N. Kallon,<sup>1</sup> T. P. M. Millard,<sup>1</sup> P. C. Diemoz,<sup>1,2</sup> and A. Olivo<sup>1,2</sup>

<sup>1)</sup>*Department of Medical Physics and Bioengineering, University College London, Malet Place, Gower Street, London WC1E 6BT, United Kingdom*

<sup>2)</sup>*Research Complex at Harwell, Harwell Oxford Campus, OX11 0FA Didcot, United Kingdom*

(Dated: 16 September 2015)

We discuss a portable Edge Illumination X-ray Phase Contrast imaging system based on compact piezoelectric motors, which enables its transportation to different environments e.g. hosting different x-ray source technologies. The analysis of images of standard samples reveals an angular sensitivity of  $270 \pm 6$  nrad, which compares well with the  $260 \pm 10$  nrad reported for previous systems based on stepper motors, demonstrating that system portability can be achieved without affecting phase sensitivity. The results can also be considered a test of the performance of the piezoelectric motors, and as such could be of interest to researchers planning their use in other imaging systems.

Keywords: X-ray phase contrast imaging, portable system, piezoelectric technology, angular sensitivity

X-ray Phase Contrast imaging (XPCi) is widely used for several applications including medical physics, biology and materials science as an alternative to absorption-based imaging techniques. While the latter provide adequate performances only when the attenuation properties of the details of interest are very different from the surrounding background, phase contrast imaging is more suitable for weakly absorbing materials<sup>1</sup>.

Among the several XPCi methods<sup>2</sup> (crystal interferometry<sup>3</sup>, analyzer-based imaging<sup>4</sup>, free-space propagation<sup>5</sup>, grating interferometry<sup>6</sup> and non-interferometric methods<sup>7</sup>), edge illumination (EI)<sup>7</sup> is one of the most promising because of its capability to be adapted with conventional laboratory sources<sup>8,9</sup>.

A common EI setup, in its implementation with divergent beams, is shown in Fig. 1. By using dedicated

algorithms<sup>10-12</sup> it is possible to retrieve information about the absorption, refraction and ultra small angle scattering properties of the sample. It has been shown that, with synchrotron radiation, EI can achieve an angular sensitivity of a few nanoradians<sup>13</sup>, while for conventional laboratory sources the achievable sensitivity was estimated to be of  $(270 \pm 5)$  nrad<sup>11</sup>. The capability of EI to work with polychromatic, divergent and incoherent x-ray beams provides access to phase contrast imaging techniques with conventional sources.

A portable and compact system was developed so that the experimental set-up can be transported to different environments (e.g. laboratories for x-ray imaging, hospitals, x-ray source facilities). The design involved the selection of miniaturized and highly precise motors, based on piezoelectric technology. Compared to the stepper motors used so far for EI experiments at the University College London (UCL) and at various synchrotron facilities, the piezo-motors are lighter and more compact, which makes them more suitable for transportation and quick set-up in different environments.

The performances of two systems, one based on stepper motors by Newport (Irvine, California, USA) and another one based on piezo-motors by SmarAct (Oldenburg, Germany), is investigated in this paper. Images of wires of different materials and thickness are shown, with the aim of comparing the angular sensitivity of the two set-ups. The results of these tests can thus be of interest to the field of XPCi and more generally, to those fields in which optical elements have to be positioned with high accuracy.

Our aim was to develop a portable, light and compact system. The masks were mounted on stacks of motors to allow for accurate alignment and movement. A dedicated LabView code was used to remotely control the devices and was integrated with the data acquisition software via a TCP/IP connection.

Motors constitute an essential part of an EI set-up

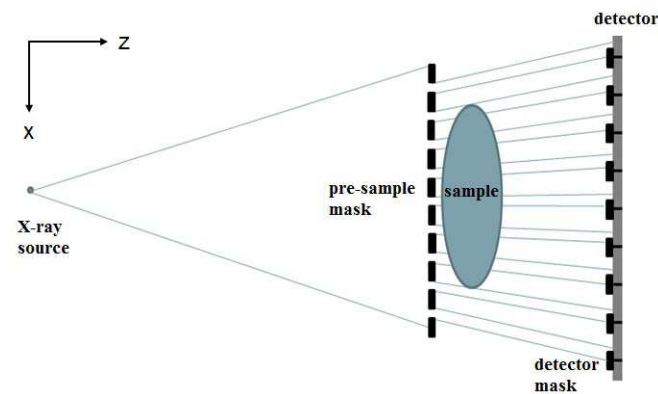


FIG. 1. EI set-up: a pre-sample mask is used to collimate and separate the x-ray beam into several beamlets; a detector mask, placed in front of the detector pixels, is used to stop part of the incoming radiation.

<sup>a)</sup>Electronic mail: [dario.basta.13@ucl.ac.uk](mailto:dario.basta.13@ucl.ac.uk)

because they are used in several procedures involving movements along different axes: mask alignment, illumination curve acquisition and sample dithering<sup>14</sup>.

Mask alignment is carried out every time a new set-up is implemented, with different values of parameters such as pitch and aperture width of the masks, magnification, detector pixel size, etc. The two masks, placed between source and detector as shown in Fig. 1, must be aligned on the optical axis in such a way that both their projected pitches match the detector pitch. While in principle the full alignment procedure requires an adjustment for all six degrees of freedom, in practice for a system which employs 1D masks only, translations along the x and z directions and rotations around z are strictly required<sup>14</sup>.

The illumination curve is the variation in detected intensity as a function of the displacement between the two masks along the transverse direction x. With the sample out of the field of view, the pre-sample mask is shifted in several steps along the x direction, resulting in different illumination levels for the detector pixels. At each mask displacement, the intensity of the radiation impinging on each pixel is recorded, leading to an intensity profile similar to the rocking curve in analyzer based imaging<sup>15</sup>. The experimental points can be fitted with an analytical function in order to extract important parameters (offset, amplitude, centroid and standard deviation). By comparing this values to those obtained when a sample is present, information about absorption, refraction and ultra small angle scattering caused by the sample can be retrieved via a dedicated algorithm<sup>12</sup>. Fig. 2 shows an example of illumination curve, with three mask displacements corresponding to three different points.

Dithering in this case means that multiple images are taken at several sub-pixel displacements of the sample along the x direction (see Fig. 1), with a total travel range of one mask period. All these images are taken while keeping the relative displacement between the two masks fixed (i.e. at the same illumination level) and then recombined to obtain one with increased spatial resolution (determined by the dithering step, rather than by the pixel size<sup>16,17</sup>). All the three procedures involve motion accuracy of a few  $\mu\text{m}$  for translations and of a few mrad for rotations<sup>14</sup>. For this reason, we selected positioners based on piezoelectric technology, which makes them compact, light and highly precise. They are a few centimetres high and weigh a few hundred grams (around one order of magnitude smaller and lighter than previous stepper motors). The full compact system is composed of: a stack of three motors (two SLC 1750-M-E linear translators and a SGO 60.5-M-E goniometer) equipped with microsensors, used to move the detector mask; a stack of three motors (two SLC 1750-S linear translators and a SGO 60.5-S goniometer) equipped with nanosensors, used to move the sample mask; an SLC 24120-M-E linear translator equipped with a microsensor, used to move the sample. A Labview

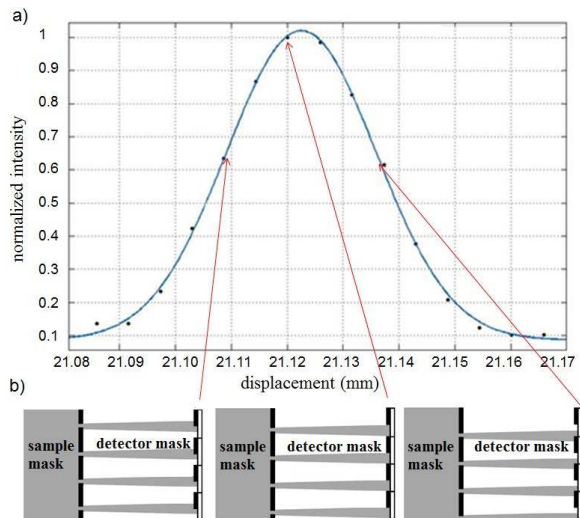


FIG. 2. (a): illumination curve; (b): pre-sample mask positions corresponding to specific points on the curve, as highlighted by arrows.

GUI interface enables the operator to directly drive the motors, while an IDL script enables their automated control during the acquisition.

Preliminary tests on a first stack of motors equipped with microsensors allowed us to evaluate the software procedure when moving the motors to absolute positions. Distributions of the discrepancies between expected and retrieved positions were obtained, resulting in a mean value consistent with 0, and with standard deviations of  $0.13 \mu\text{m}$  for the linear positioners and  $2.3 \mu\text{rad}$  for the goniometer: these values are comparable with the nominal resolution of the sensors ( $0.10 \mu\text{m}$  and  $1.5 \mu\text{rad}$ , respectively). A second stack of motors with nanosensors was also tested, leading to an improvement of two orders of magnitude. Estimated values for the discrepancy were consistent with 0, with a standard deviation of  $0.7 \text{ nm}$  for the linear translators and  $20 \text{ nrad}$  for the goniometer. Images of wires of different materials and thicknesses were acquired using both the original system, based on stepper motors, and the portable system based on piezo-motors. The x-ray source was a Rigaku MM007 X-ray tube with a Mo target operated at  $35\text{kV}/25\text{mA}$ , with a spot size of  $75 \mu\text{m}$ . The detector was the Hamamatsu C9732DK flat panel with a  $50 \mu\text{m}$  pixel size. The aperture width and the pitch of the pre-sample mask were  $23 \mu\text{m}$  and  $79 \mu\text{m}$ , respectively. The detector mask aperture width was  $29 \mu\text{m}$ , and the pitch  $98 \mu\text{m}$ . The source-to-object distance was  $1.6 \text{ m}$ , while the source-to-detector distance was  $2 \text{ m}$ .

Raw data for each set of acquisitions were processed with a dedicated algorithm<sup>12</sup>, which retrieves absorption, refraction and scattering signals from three input projection images. Each projection image was acquired at different positions on the illumination curve, typically one at the centre (corresponding to 100% intensity),

and the other two at 50% intensity on opposite sides. All three images consisted of 6 dithering steps, each one acquired with 5 sec exposure time. The retrieved refraction signal, and a profile along a row of detector pixels, were obtained for both systems, as shown in Fig. 3. For a quantitative comparison between the two set-ups, the angular sensitivity<sup>11</sup> was estimated. For the SmarAct system, the value of the angular sensitivity is  $(270 \pm 6)$  nrad, while for the Newport system is  $(260 \pm 10)$  nrad: the two values are thus comparable within the experimental uncertainty.

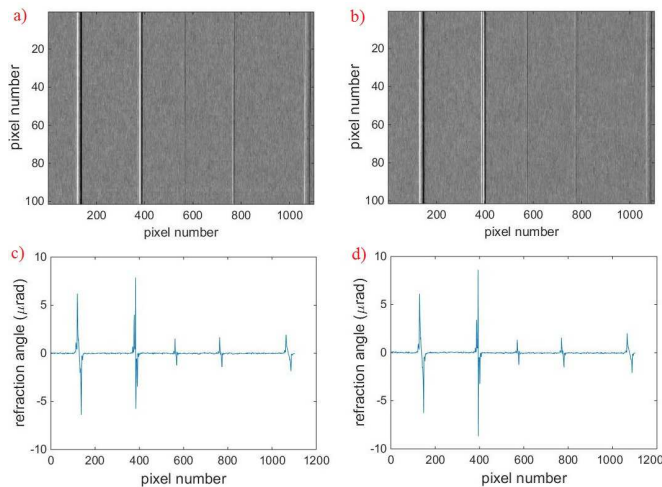


FIG. 3. Refraction images a),b) and corresponding profiles c),d) for portable and previous system, respectively.

The design and realization of a portable EI-XPCi system has been presented. The basic component are compact and light piezo-motors, which provide a good compromise between high positioning accuracy and easy transportation of the set-up. A dedicated control system based on LabView software was implemented to drive the motors in an automated way.

The performance of the portable system was quantitatively compared to that obtained by using stepper motors, used so far in previously presented EI set-ups. For both systems, the angular sensitivity in the refraction signal was extracted from images of wires of different materials and thicknesses. This provides an estimation of the smallest deviation angle detectable with both set-ups: for the portable system, a value of  $(270 \pm 6)$  nrad was obtained, while the previous system yielded a value

of  $(260 \pm 10)$  nrad.

A light and compact system based on piezo-electric motors was realized, maintaining the same sensitivity to angular deflections as that obtained so far with the system based on stepper motors. This feature, together with the capability of EI to be adapted to laboratory sources, extends the potential of the method to be used by a wider community in a more diversified range of applications and environments.

This work was supported by the UK Engineering and Physical Sciences Research Council Grant EP/I021884/1 and by the UK Science and Technology Facilities Council Grant ST/L502662/1. M.E. and P.C.D. are supported by Marie Curie Career Integration Grant within the Seventh Framework Programme of the European Union PCIG12-GA-2012-334056 and PCIG12-GA-2012-333990.

- <sup>1</sup>S.W. Wilkins, T.E. Gureyev, D. Gao, A. Pogany, and A.W. Stevenson *Nature* **384**, 335 (1996).
- <sup>2</sup>A. Bravin, P. Coan, and P. Suortti, *Phys. Med. Biol.* **58**, R1-R35 (2013).
- <sup>3</sup>U. Bonse and M. Hart, *Appl. Phys. Lett.* **6**, 155 (1965).
- <sup>4</sup>T. Davis, D. Gao, T. Gureyev, A. Stevenson, and S. Wilkins, *Nature (London)* **373**, 595 (1995).
- <sup>5</sup>A. Snigirev, I. Snigireva, V. Kohn, S. Kuznetsov, and I. Schelokov, *Rev. Sci. Instrum.* **66**, 5486 (1995).
- <sup>6</sup>C. David, B. Nöhammer, H. Solak, and E. Ziegler, *Appl. Phys. Lett.* **81**, 3287 (2002).
- <sup>7</sup>A. Olivo, F. Arfelli, G. Cantatore, R. Longo, R. Menk, S. Pani, M. Prest, P. Poropat, L. Rigon, G. Tromba, E. Vallazza, E. Castelli, *Med. Phys.* **28**, 1609 (2001).
- <sup>8</sup>A. Olivo and R. Speller, *Appl. Phys. Lett.* **91**, 074106 (2007).
- <sup>9</sup>P.R.T. Munro, K. Ignatyev, R.D. Speller, and A. Olivo, *Opt. Express* **18**, 19681 (2010).
- <sup>10</sup>P.R.T. Munro, K. Ignatyev, R.D. Speller, and A. Olivo, *Proc. Natl. Acad. Sci. U.S.A.* **109**, 13922 (2012)
- <sup>11</sup>P.C. Diemoz, C.K. Hagen, M. Endrizzi, and A. Olivo, *Appl. Phys. Lett.* **103**, 244104 (2013)
- <sup>12</sup>M. Endrizzi, P. C. Diemoz, T. P. Millard, J. L. Jones, R. D. Speller, I. K. Robinson, and A. Olivo, *Appl. Phys. Lett.* **104**, 024106 (2014)
- <sup>13</sup>P.C. Diemoz, M. Endrizzi, C.E. Zapata, Z.D. Pešić, C. Rau, A. Bravin, I.K. Robinson, and A. Olivo *Phys. Rev. Lett.* **110**, 138105 (2013)
- <sup>14</sup>T. Millard, M. Endrizzi, K. Ignatyev, C. Hagen, P. Munro, R. Speller, and A. Olivo *Rev. Sci. Instrum.* **84**, 083702 (2013)
- <sup>15</sup>D. Chapman, W. Thomlinson, R.E. Johnston, D. Washburn, E. Pisano, N. Gmur, Z. Zhong, R. Menk, F. Arfelli, and D. Sayers *Phys. Med. Biol.* **42**, 2015-2025 (1997).
- <sup>16</sup>K. Ignatyev, P. R. T. Munro, R. D. Speller, and A. Olivo, *Rev. Sci. Instrum.* **82**, 073702 (2011).
- <sup>17</sup>P.C. Diemoz, F.A. Vittoria and A. Olivo *Opt. Express* **84**, 15514 (2014)